Unsaturated flow through fracture networks: Evolution of liquid phase structure, dynamics, and the critical importance of fracture intersections

Robert J. Glass,[1] Michael J. Nicholl,[2] Harihar Rajaram,[3] and Thomas R. Wood[4]

Received 27 January 2003; revised 2 May 2003; accepted 8 September 2003; published 17 December 2003.

[1] Experiments and analyses are presented to elucidate the critical control of fracture intersections on the evolution and dynamics of the liquid phase structure within unsaturated fracture networks in impermeable media. Phase structure was visualized within a thick vertical sheet of broken glass where the breaks constituted the fracture network. The critical system parameters, applied flow rate (viscous forces) and initial condition, were varied in a series of experiments. When initially dry, individual fracture intersections acted as capillary barriers and created a repeated dynamic from which a network-scale ''slender-ladder'' phase structure emerges that is composed of pools above each intersection joined by fingers or ''tendrils'' below. At low-flow rates, pulsation is found at intersections, within fingers, and along horizontal fractures. In some cases, pulsation extends to larger volume ''cascade'' events where several intersections act in concert. At higher-flow rates, viscous forces remove pulsation. Reinvasion upon drainage demonstrates that when initially wet, the capillary barrier behavior of the individual fracture intersections vanishes and intersections are rapidly spanned. This marked hysteretic response tends to guide flow and cause pathway persistence from one event to the next. *INDEX TERMS:* 1829 Hydrology: Groundwater hydrology; 1875 Hydrology: Unsaturated zone; 1832 Hydrology: Groundwater transport; *KEYWORDS:* fractured rock, fracture intersections, capillary barrier, fingering, preferential flow, pulsation, hysteresis

Citation: Glass, R. J., M. J. Nicholl, H. Rajaram, and T. R. Wood, Unsaturated flow through fracture networks: Evolution of liquid phase structure, dynamics, and the critical importance of fracture intersections, *Water Resour. Res.*, *39*(12), 1352, doi:10.1029/2003WR002015, 2003.

1. Introduction

[2] Unsaturated and two-phase flow through fractured rock remains a topic of interest with applications in the fields of radioactive waste disposal, contaminant transport, geothermal energy production, and fossil fuel extraction. Within the context of field-scale transport through unsaturated fractured rock, focused transport pathways are a common occurrence [e.g., *Russell et al.*, 1987]. There is also a body of field evidence that shows rapid and deep penetration of fractured vadose zones by both meteoric water [e.g., *Fabryka-Martin et al.*, 1996; *Davidson et al.*, 1998], and fluid from ponded infiltration experiments [e.g., *Glass et al.*, 2002b]. Additionally, several recent field experiments have shown temporal and spatial dynamics suggestive of complex unsteady behavior, sometimes under conditions of long-term steady supply or ponding [e.g., *Dahan et al.*, 1999; *Faybishenko et al.*, 2000; *Podgorney et al.*, 2000]. While many of these large-scale field results could be inferred from physical processes acting in single fractures under conditions of unsaturated and two-phase flow [*Glass et al.*, 1995, 2001; *National Research Council*, 1996], network effects have yet to be considered in detail.

[3] In an effort to understand how single fracture processes manifest themselves in the context of a fracture network within porous rock, *Glass et al.* [2002a] conducted mesoscale (1–2 m) experiments within an unsaturated fracture-matrix network composed of an uncemented wall of porous bricks. In their experiment, multiple flow pathways evolved that were heavily controlled by processes acting within the fracture network, demonstrating the dual nature of fractures as both primary flow conductors, and as barriers to fluid transfer between adjacent matrix blocks. For flow within the fracture network itself, water was observed to move rapidly along fractures and then wait at intervening intersections, thus suggesting that fracture intersections behaved as capillary barriers. At intersections, flow sometimes continued downward and sometimes turned sideways, emphasizing the control that intersections place on pathway formation, and suggesting their possible influence as a ''switch.'' Outflow from the fracture-matrix network contained fluctuations/pulsations at scales ranging from minutes to months, both along individual pathways, and involving switching between alternate pathways.

[4] Pulsation along gravity-driven fingers within individual nonhorizontal fractures was reported by *Nicholl et al.*

[1]Flow Visualization and Processes Laboratory, Sandia National Laboratories, Albuquerque, New Mexico, USA.
[2]Mining and Geological Engineering, University of Idaho, Moscow, Idaho, USA.
[3]Department of Civil, Environmental, and Architectural Engineering, University of Colorado, Boulder, Colorado, USA.
[4]Idaho National Engineering and Environmental Laboratory, Idaho Falls, Idaho, USA.

0043-1397/03/2003WR002015$09.00

[1993a, 1993b], and subsequently studied by *Su et al.* [1999, 2001]. Such fingering and pulsation is also clearly important in heat driven flows within individual nonhorizontal fractures, as studied by *Kneafsey and Pruess* [1998]. Additionally, pulsation has been documented in individual horizontal fractures during both concurrent gas-liquid flow [*Persoff and Pruess*, 1995] and slow nonwetting displacement [*Amundsen et al.*, 1999]. However, in the mesoscale unsaturated fracture-matrix network considered by *Glass et al.* [2002a], fluctuations in outflow were much larger and less frequent than could be attributed to a pulsation dynamic within individual fractures. Because the phase structure (liquid/gas) within the fracture-matrix network could not be visualized, they could only speculate on the cause of outflow dynamics. They suggested that such a response could arise within the network from fracture intersections acting as integrators [see *Wood et al.*, 2002] or through a cascade process that linked volumes distributed within the network or both. They also suggested that pathway switching was a result of pulsation at fracture intersections.

[5] The objective of this paper is to further elucidate the processes that control liquid phase structure growth and dynamics within unsaturated fracture networks. In particular, we focus on the critical behavior of fracture intersections and their influence on the larger-scale behavior of the network. To accomplish this, we designed a transparent experimental system in which a controlled fracture network was imposed on a thick sheet of glass. This transparent system allowed us to directly observe liquid phase structure evolution and dynamics as an experiment progressed. Because approximately orthogonal fracture sets were created sequentially, individual fracture intersections showed slight offset, such as expected in natural fracture networks. In this system, we conducted a series of controlled flux infiltration experiments where water was supplied to the central fracture at the top of the network. First, we supplied water at a slow steady rate to the initially dry network. After following the initial invasion process and subsequent dynamics in detail, we then increased the supply rate to consider the influence of viscous forces on the flow pathway structure and dynamics. Finally, after interrupting water supply and allowing the fracture network to drain to a stagnant state, reinvasion of the prewetted network was considered under both the highest and lowest flow conditions.

[6] Experimental results and analysis demonstrate the critical control of fracture intersections on the development of network-scale phase structure, dynamics, and the resulting transport pathway. Four critical observations are distilled. First, the invasion of individual initially dry fracture intersections follows a repeated dynamic that tends to create a local ''pool and finger'' structure with filled, but nonconducting horizontal fractures on either side of the intersection. Second, this local structure is linked together primarily in the vertical, and forms a ''slender-ladder'' structure. This system-scale structure emerges due to the directional dependence of the local invasion process at individual intersections where a slight offset occurs. Third, at low-flow rates, pulsation can be found at intersections, within fingers, and along horizontal fractures, as well as organized into larger-scale cascade events where individual pulses act in concert. At higher-flow rates, such pulsation is stabilized by viscous forces. Fourth, there is a strong tendency for pathways to persist over at least the time periods of our experiment. The initial or current phase structure tends to guide flow due to significant hysteresis in the intersection invasion pressures. However, at low-flow rates and at long times, the possibility remains that pulsation can create new flow paths through the fracture network.

2. Experimental System

[7] We developed a simple experimental system that allows us to observe unsaturated flow processes acting within a fracture network. The experimental system is based on a two-dimensional network of controlled breaks (fractures) in a thick sheet of glass (Figure 1). The glass is broken along preselected lines by laying a resistive wire on top of the glass, and then heating the wire electrically. Wire shims are used to control the gaps that form individual fractures within the thick fractured glass (fractures span the full thickness or ''width''). The network is held together inside a frame, with a piece of unbroken ''boundary'' glass on each side to form a barrier to fluid flow and vapor transport (see inset for horizontal cross section of cell in Figure 1). To constrain the wetting fluid (water here) within the 2D network, the ''boundary'' gap separating the thick fractured glass from the boundary glass is much larger than the fracture gaps.

[8] The fracture network fabricated for our study was designed to be a set of imperfect, and slightly wavy vertical and horizontal fractures on an ~5 cm grid within a 60 cm tall by 30 cm wide piece of 1.9 cm thick glass (see Figure 1). We chose this configuration to maximize behavioral differences due to orientation within the gravitational field (i.e., vertical vs. horizontal fractures). The vertical fractures were broken first, followed by individual breaks along their lengths to form the horizontal fractures. This sequence created fracture intersections where the vertical fractures are throughgoing (lined up with no offset), while the horizontal fractures are offset by 0.5–5 mm (see inset of high-resolution portion of network in Figure 1). Note that to minimize inflow boundary effects, we designed the network so that the first fracture segment along the flow path would be twice as long (~10 cm) as the other segments. Before assembly, each piece of glass forming the network was cleaned with a concentrated sulfuric acid solution (Nochromex™) to homogenize surface properties as much as possible.

[9] The network was assembled horizontally. To begin, a piece of 0.5 mm thick plastic sheeting was lain on top of the front boundary glass; removal of the plastic at the end of assembly provided the front boundary gap. Individual pieces of the thick fractured glass were then assembled on top of the plastic with spacers between (see Figure 1). The spacers used to establish the gaps (i.e., fracture apertures) within the network were formed of 0.1 mm diameter precision stainless steel wire (STD ~ 0.001 mm). A small curled piece of wire ~3–5 mm across was dropped into the middle of each fracture, and allowed to rest on the plastic. Two additional pieces of wire were then inserted a distance of ~2 mm into the fracture, one on either side of the midpoint ~3–4 cm apart, and then bent and taped to the back side of the thick fractured glass (see inset for typical placement of wire shims in Figure 1). This arrangement of wire shims provided three areas of contact within each fracture and thus on application of clamping pressure from the net-

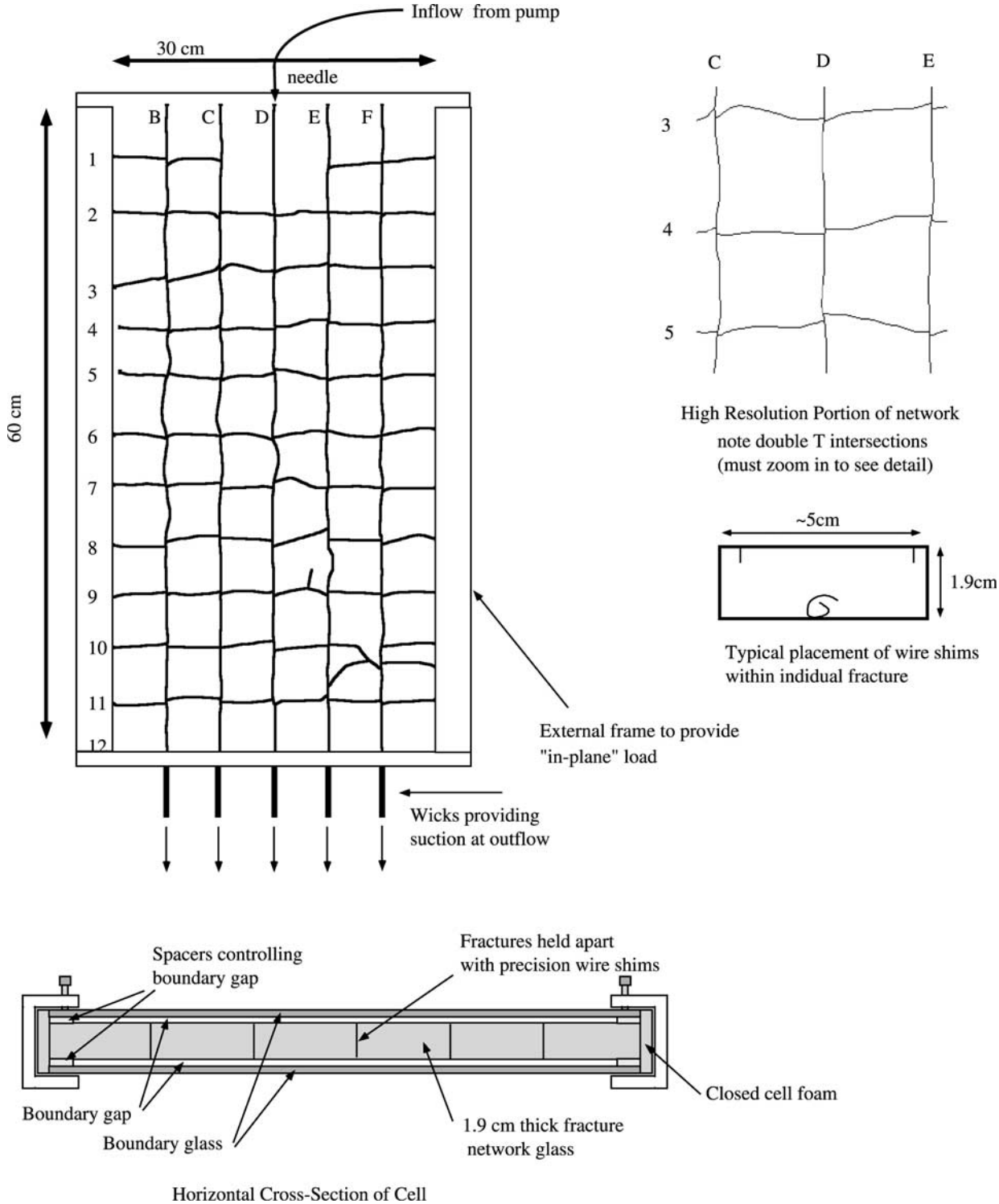

Figure 1. Experimental system. The experimental system is formed by a network of controlled breaks in a sheet (30 cm wide × 60 cm tall) of 1.9 cm thick glass. Each intersection is composed of a throughgoing vertical fracture with two abutting horizontal fractures that are slightly offset in the vertical to form two sequential ''T'' subintersections (see inset showing a high-resolution portion of the network). Three precision wire shims (0.1 mm, STD 0.001 mm) are placed within each fracture to maintain and control the gap (see inset showing typical placement of wire shims within individual ~5 by 1.9 cm fractures). The network is held together inside a load frame, with a piece of unbroken boundary glass on each side (see horizontal cross section of cell). The boundary glass sheets are held at a controlled distance from the network, so that the intervening gap serves as a barrier to the wetting phase (water), while the glass itself minimizes evaporative losses. Water is supplied at the top of the network in the center fracture and exits out the bottom through braided fiberglass wicks.

work edges, yielded a mechanically stable system. Once the back boundary glass was installed, the system was clamped together and oriented vertically in front of a diffuse light source. The plastic sheet between the front boundary glass and the thick fractured glass was then pulled out the top to yield the front boundary gap. To provide for top and bottom boundary conditions, end plates were then sealed to the system. The top plate allowed for insertion of the inflow needle, while the bottom plate provided openings for 5 cm long prewetted wicks (~height of each glass block) installed at the bottom of each fracture. To reduce evaporative losses, air could only enter/exit the system through holes for the outflow wicks and inflow needle.

[10] Flow was supplied to the top of the network through a needle inserted into the top middle fracture (labeled D in Figure 1) with a peristaltic pump designed for long term, low flow, near constant supply (Masterflex™ 7521–50 with eight roller head 7519, two cassettes mounted in opposite directions, and 0.25 mm ID tubing). Supply rate was monitored with an electronic balance ±0.001 g accuracy). Red dye (FD&C red #3) was added to the water to increase visibility. CCD video cameras were set up at a variety of angles to record water advance into the network. Because of our desire to investigate the high interfacial tension air-water system, with its commensurately high density and thus refractive index contrast, reflection and refraction of light at breaks in the glass posed difficulties for visualization of fluids within the network (see Figure 2 as an example). Thus camera positions were often moved to capture action over the course of the experiment. During the initial network invasion, the extent of the wetted structure was recorded in time directly on the front piece of glass. These marks were later used to provide scale for measurements taken from video or photographs.

[11] The contact areas provided by the shims were very small and disconnected, thus their influence on phase invasion was minimal. With this design, fracture apertures across the network were nearly the same, but would have had some variability due to assembly. Additionally, during phase invasion, we noted that invasion structures within individual fractures were often irregular. Thus there may have been some aperture variability within individual fractures induced by slight misalignment of the perfectly matched, but wavy broken surfaces. It is also possible that the irregular phase structures were due to local contact angle variability along the glass surfaces. To characterize the properties of a typical fracture, we performed capillary rise and capillary drainage experiments on 5 separate 15 cm tall fractures cleaned and assembled similarly to those in the network experiment. In the capillary rise experiment, the bottom of an initially dry fracture was placed in contact with a body of red dyed water such as we used in the experiment. Water rose into the fractures to an average height of ~4 cm (range 3 to 5 cm). In the capillary drainage experiment, a fracture was first water saturated, and then placed in contact with a body of water into which it drained. The wetted structure below ~6 cm (range 5 to 7 cm) spanned the full fracture with partial desaturation above.

3. Experiments

[12] Our experimental design varied the system parameters of applied flow rate (viscous forces) and initial condition,

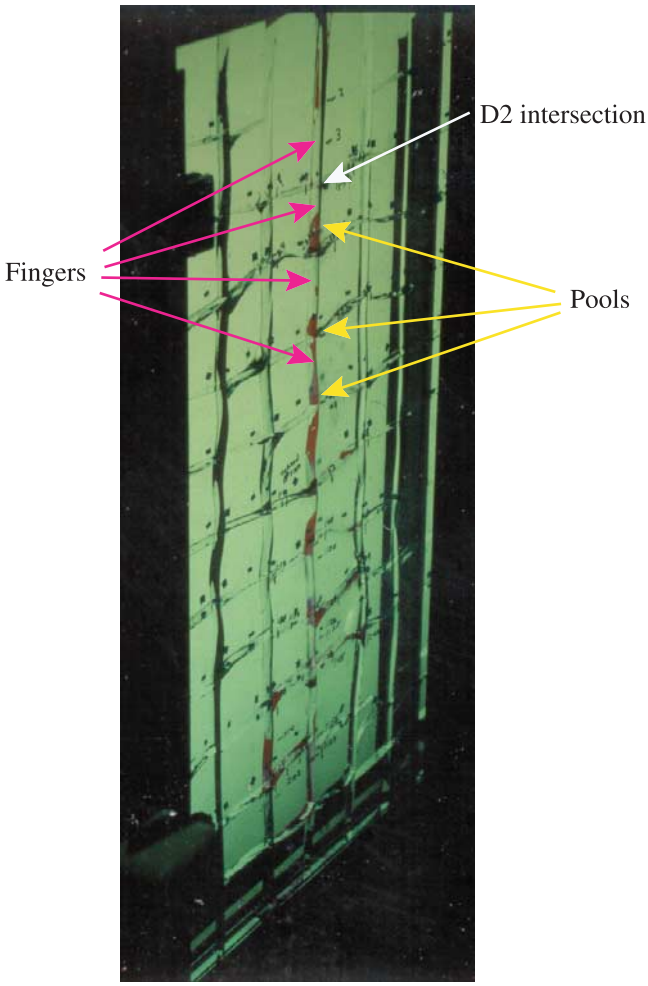

Figure 2. Photograph of phase structure at 3.72 hours. Taken from the left and slightly above the network, this photo illustrates the "slender-ladder" pool and finger structure within the vertical fractures. Water is seen as red. From this angle, water within the horizontal fractures cannot be seen. Other dark regions are due to reflection and refraction of light from the diffuse backlight, and emphasize the difficulty of observing phase structure within this fractured system.

both thought to be important in the formation of phase structure and the subsequent stability of flow pathways within the network. We first followed the invasion of water within the initially dry network at a low rate (0.019 mL/min), where viscous forces would be small relative to capillary and gravity forces (section 3.1). After water had begun to drip out of the wicks at the bottom of the network, we then observed the dynamics and further evolution of the phase structure over the course of a ~24 hour period (section 3.2). To consider the stability of the established phase structure under increased viscous forces, we increased flow in a series of steps. At each step we approximately doubled the previous flow rate (0.031, 0.11, 0.18, and 0.36 mL/min), then observed the phase structure for ~24 hours (section 3.3). At the highest flow rate (0.36 mL/min), the flowing phase structure occupied a portion of the fracture network at near saturation. The rest of the network remained dry, and the near saturated portion

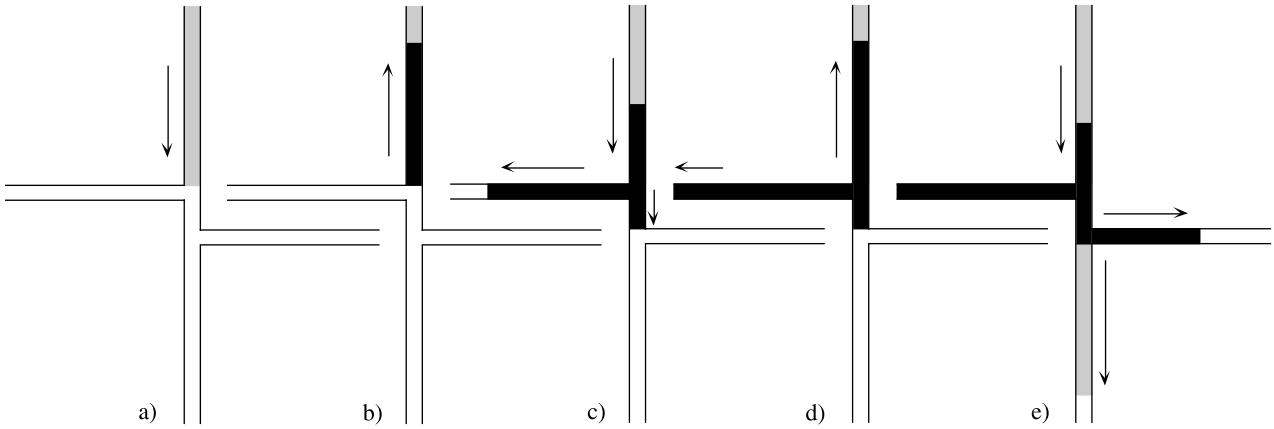

Figure 3. General invasion process at the double T intersection. The double T intersections in our network were invaded in a series of steps. In this idealized caricature, white indicates air filled, shading indicates a finger that partially fills the fracture, and solid indicates a fracture filled with water to entire width (with some air entrapment). Capillary-induced curvature is not drawn. (a) Water fingers down to the intersection. (b) Pool backfills above the first T. (c) Upper T breaches, water enters the vertical fracture below and upper horizontal fracture, while pool height decreases. (d) Upper horizontal fracture fully fills, pool height again rises above first T. (e) Lower T breaches, water enters vertical fracture below as a finger and partially fills the lower horizontal fracture.

stayed within the 2D network (i.e., water pressure was insufficient to enter the wider boundary gaps on either side of the thick fractured glass network). At the end of this sequence, we then considered the influence of an initial drained phase structure on the subsequent reinvasion of water (section 3.4).

3.1. Initial Invasion at the Lowest Flow Rate

[13] Initial invasion of the dry network (0.019 mL/min) was recorded in detail. Below the entry point at the needle, water moved downward as a finger (~2–4 mm wide).The first cm of the finger occurred as a film on the side of the fracture contacted by the needle. Below this small region of film flow, the water spanned the aperture, contacting both fracture walls. We note that this was the only occurrence of film flow in the entire experimental sequence, and that this film was replaced by aperture spanning flow from the needle within the first 2 hours of the experiment. When the finger reached the first fracture intersection (D2 in Figure 1), it began to back fill the fracture upward to its full width (front to back of the thick fractured network glass). This region we call a ''pool'', as it forms above an intersection that acts as a capillary barrier. We define ''pool height'' by the distance between the intersection and the location above which the fracture is no longer fully filled. At intersection D2, the pool rose to a height of ~4 cm before the capillary barrier was breached at 0.15 hours, after which, pool height decreased to ~2 cm. As the intersection breached, the pool above began to drain into both the vertical fracture below, and the upper horizontal fracture to the left. In the vertical fracture, downwards water invasion stopped at the lower horizontal fracture to the right (next capillary barrier), meanwhile, the upper horizontal fracture continued to fill. As height of the draining pool neared 2 cm, invasion of the horizontal fracture slowed, but continued until the fracture was entirely full, with some entrapped air due to capillary fingering. At this point, the level in the pool above intersection D2 began to once again rise. When the pool reached a height of ~3 cm, water broke both into the lower right horizontal fracture and concurrently formed a finger in the vertical fracture below (0.3 hours). As the finger grew downward in the vertical fracture, flow into the lower right horizontal fracture was curtailed such that it did not fully fill, and the pool height above D2 dropped and stabilized at ~2 cm. When the downward growing finger reached the next intersection (D3), it stopped and began backfilling the fracture, thus creating the next pool.

[14] This intersection invasion process, described in detail for the first intersection at D2, repeats itself over and over as the network is invaded. Figure 3 illustrates this invasion process in a series of drawings for an idealized intersection. Water first fingers down to a fracture intersection from above (Figure 3a) and pools above the fracture intersection until pressure at the intersection reaches its breach point (Figure 3b). The details of the fracture intersection then come into play. Since the fracture intersections were lined up (throughgoing) only in the vertical, with the horizontal fracture slightly offset, each intersection was in essence composed of two adjoining ''T'' subintersections that create a two barrier sequence (see inset of high-resolution portion of network in Figure 1). When the first barrier breaches and the pool height begins to drop, the adjoining top horizontal fracture starts to fill as does the small zone (~0.5–5 mm) between the top and bottom T barriers (Figure 3c). Both of these zones fill entirely, followed by a delay while the pool height above increases, and pressure builds up at the lower T barrier (Figure 3d). When the second breach occurs, the pool height drops and water moves both into the side horizontal fracture and as a finger below. The hanging column imposed by the finger decreases the pressure at the intersection, and curtails the further invasion of the lower horizontal fracture (Figure 3e). In some cases, we found the lower horizontal fracture to hardly fill. The finger in the vertical fracture continues down to the next major intersection where the process begins again.

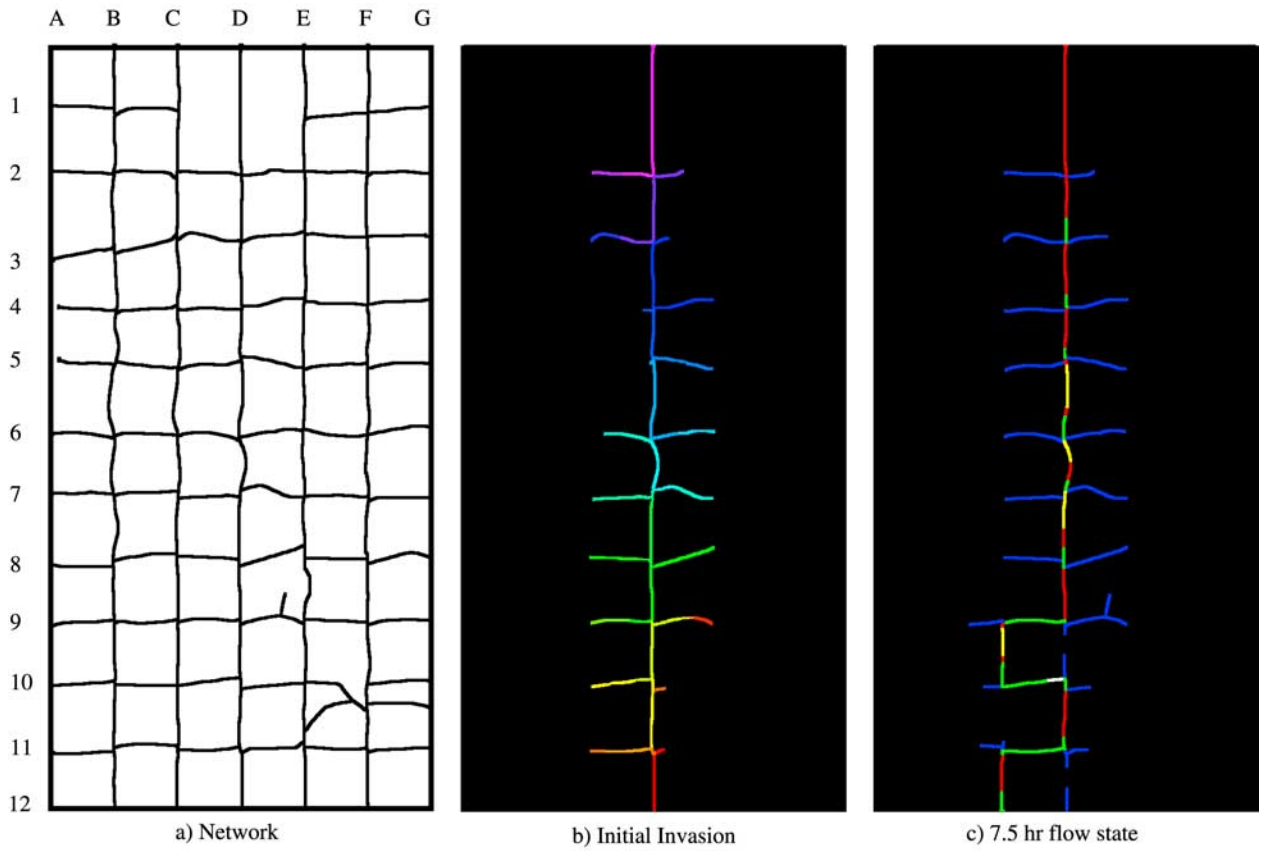

Figure 4. Drawings of invasion structure and flow state over the experimental sequence: (a) Fracture network with letters (A–G) and numbers (1–12) to designate fracture intersections. (b) Initial invasion order, with the color sequence purple-blue-green-yellow-orange-red designating time up to 2.92 hours when the network was spanned from top to bottom. (c) Flow state at 7.5 hours, with color representing zones where the full width of the fracture was filled and conducting, such as found in pools and some horizontal fractures (green), nonconducting zones that were filled to full width (blue), zones occupied by fingers that do not span the full fracture width (red), zones where pulsation occurred as a finger formed and then snapped repeatedly (yellow), and a single zone where pulsation occurred within a horizontal fracture (white).

[15] As the invading water phase progressed downwards, the magnitude of pool dynamics varied from intersection to intersection. At some intersections the pool drained dramatically after the barrier was breached (as described at D2 above), while at other intersections there was little to no change in pool height during drainage. Additionally, the phase structure local to the intersection sometimes expanded and then contracted in the horizontal fractures to the side. In the top half of the network, the phase structure stabilized as the intersection invasion process advanced to the next intersection. However, pulsation, where the finger below an intersection repeatedly snapped and then reformed, began to occur between intersections D7 and D8. This pulsation also involved the left horizontal fracture (lower horizontal fracture at the intersection) at D7 as well. We note that while the peristaltic pump may have introduced slight pulsation to the inflow, at this flow rate, any such signal was below the detection limits of our monitoring system. Regardless, close scrutiny of the phase structure within the cell above the highest point of pulsation suggested steady flow. Considering viscous damping within the unsaturated phase structure within the network, we believe it is very unlikely that any signal in the inflow forced pulsation within the network. Instead, the pulsation arises naturally within the network on its own. Water reached the bottom of the network connecting the string of intersections within the middle vertical fracture (D) at 2.57 hours and entered the prewetted wick at D12. Figure 4b shows the temporal evolution of the flow pathway during the initial invasion period with color representing time.

3.2. Dynamics Within the Low-Flow Structure Subsequent to Initial Invasion

[16] Over the few hours following network breakthrough, the phase structure became increasingly complex and dynamic. At 2.93 hours, a finger grew downward from the C11 intersection and entered the wick at C12, thus dividing the flow path at D11 with outflow at both C12 and D12. At 3.32 hours, a downward growing finger formed from C9 and grew to C10. This finger then snapped off, reformed, and continued in this pulsating mode. Then at 3.37 hours, the finger between D9 and D10, as well as between D11 and D12, snapped and did not reform.

[17] From 3.4 hours until 7.6 hours, the flow path did not change, however, the entire structure showed temporal fluctuation. A photograph of the phase structure taken from

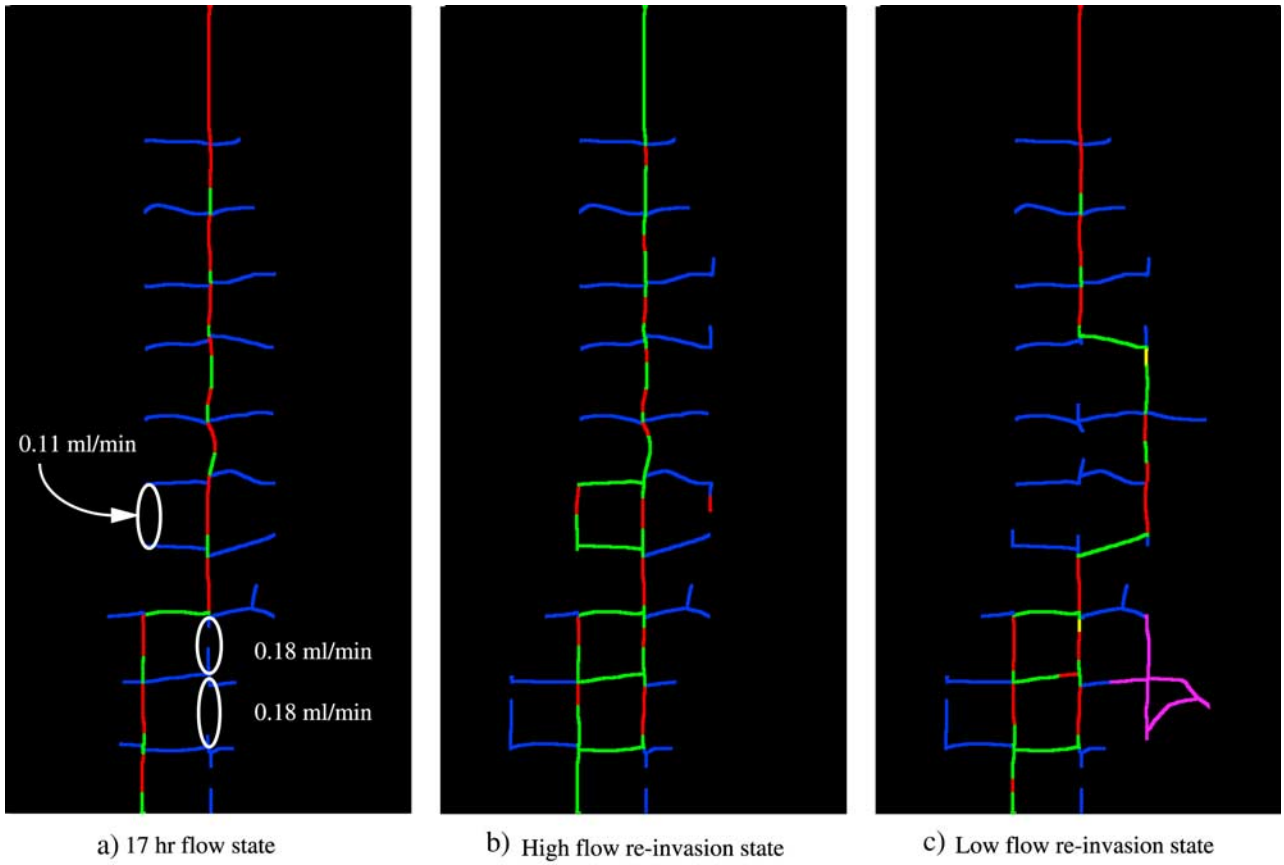

Figure 5. Drawings of invasion structure and flow state over the experimental sequence. (a) Flow state at 17 hours, with color representing state zones as in Figure 4c, white circles indicate additional connections formed between intersections as flow rate was sequentially increased (see text). (b) Flow state after high-flow reinvasion, with color representing flow state zones as in Figure 4c. (c) Flow state after low-flow reinvasion, with color representing flow state zones as in Figure 4c and purple designating a flow excursion that took place on day 4 of this final experiment.

the left side at 3.72 hours (Figure 2) shows the series of pools connected by fingers within the network. In many cases, the fingers have reduced their width to form fine "tendrils". We can also see in the photo that the pool at D2 has disappeared and been replaced with a throughgoing finger. While pool heights throughout the network were stable, in some places the fingers between pools pulsed, either fully connecting and disconnecting or simply widening and narrowing in time. Figure 4c illustrates the flow state for this period designated by: (1) zones where the full width of the fracture was filled and conducting such as found in pools and some horizontal fractures (green); (2) zones occupied by fingers that do not span the full fracture width (red); (3) zones where pulsation occurred as a finger formed and then snapped repeatedly (yellow); and (4) nonconducting zones such as occurred where horizontal fractures dead-end off a fracture intersection (blue). While most horizontal fractures were nonconducting, three were integral to the flow path: D9 to C9, C10 to D10, and D11 to C11. We also found that the sequence of finger zones from D5 to D6, D6 to D7, D7 to D8, and C9 to C10 along the pathway all pulsed in concert. During this group dynamic or "cascade" event, fingers were established rapidly in sequence from top to bottom. Each finger would then narrow to a fine tendril. The tendrils would then snap, once again in sequence from top to bottom. A portion of the horizontal fracture between C10 and D10 (designated by white in Figure 4c) also participated in this cascade event and showed a rather large volume change (excursions on the order of 1 cm full width).

[18] Between 7.6 hours and 17 hours, the flow path once again changed, with flow between D10 and D11 replaced with flow between C10 and C11. After this path change, the flow structure stabilized, with no visible pulsation and was composed of a series of pools connected through very narrow (~0.1 mm) tendrils (Figure 5a). This quiescent structure was maintained up to 27.1 hours, when the sequence of increasing flow rates began.

3.3. Increasing Flow Rates and Subsequent Drainage

[19] At 27.1 hours, we increased flow to 0.031 mL/min, noting no change in flow path, and only a slight widening of some tendrils near the top of the network. Our second flow increase to 0.11 mL/min at 51.8 hours produced additional tendril widening, as well as the formation of a new connection within the flow structure between C7 and C8 (another finger and pool, circled on Figure 5a). At our next flow increase (0.18 mL/min at 147 hours), the flow structure formed two other connections, from D9 to D10 and D10 to D11 (each finger and pool, circled on Figure 5a). The

structure also changed throughout, exhibiting deeper pools and wider or sometimes multiple thin tendrils. At 173.1 hours, we increased flow to our highest value of 0.36 mL/min. At this point, no additional connections were made, however, once again, tendrils widened and pools deepened. In the upper half of the cell where a single pathway carried all the flow, the liquid phase structure extended the full width of the individual fractures (to the edges of the boundary gap). Because the boundary gap is open, this liquid phase structure suggests a saturated state that is in tension or possibly at slight positive pressure. Throughout the phase structure we could see significant entrapped air, especially within zones that had originally contained single fingers. The following day, after verifying that the flow structure was steady, we shut the pump off and allowed the system to drain. The draining structure within each vertical fracture first narrowed to a fine tendril with a shallow pool below. Tendrils eventually snapped, leaving the pools disconnected. For horizontal fractures, only a few small zones drained, most being left in their full width configuration. During this drainage process, some, but very little, pulsation was observed.

3.4. Reinvasion of the Prewetted Network

[20] Once the drainage structure had relaxed to stagnation, we began our reinvasion sequence of the prewetted network. On restarting flow at 0.36 mL/min, the network was quickly spanned (between 1 and 2 minutes) as fingers formed and grew downward sequentially at each intersection. No increase in pool height occurred at each intersection before it was breached, however, pool heights increased immediately afterwards and rose to approximately the same positions as in the earlier high-flow case. The flow state after drainage and reinvasion followed the same path as before, with one additional connection between D10 and D11 (Figure 5b). However, five additional excursions into adjoining intersections occurred along horizontal fractures connected to the main pathway. At these intersections, water generally invaded either upwards or downwards, rising in the adjoining vertical fracture if the connecting horizontal formed the upper T (E4, E5, and B11) or descending if it was the lower T (E7). However, at B10, water rose only to span the distance from the lower to the upper T. While not contributing to the transport pathway, these additional branches increased the complication of the liquid phase structure within the fracture network. After a day with no signs of pulsation or pathway changes, we discontinued flow.

[21] After allowing the system to drain to a stagnant state, we once again reestablished flow, now at a final low rate near to the initial value (0.021 mL/min). While network invasion followed the original pathway in the top and bottom thirds of the network, it veered to the right at D5 to E5, E6, E7, E8 and then back to D8 before spanning the network at 0.75 hours (Figure 5c). We found that when the flow stayed within the originally wetted fractures, nearly no pool height changes occurred, and the intersections were connected quickly with downward growing fingers between (similar to that found at the previous high-flow rate, prewet invasion). However, during the side excursion into the initially dry E fracture (E5 to E7), the wetting pattern reverted to that described during initial network invasion in section 3.1 above. During the night of the 4th day, a small excursion occurred from D9 to E9, E10, D10, F10 and E11, all of which was stagnant by morning (see excursion on Figure 5c). Pulsation began very early on the first day below E5 and D9, where it continued on and off for the next 17 days, after which the experiment was terminated.

4. Analysis and Discussion

[22] Our experiment was designed to elucidate the processes that control phase structure growth and dynamics within fracture networks. Through the use of a transparent experimental system, we were able to observe system behavior as we varied the critical control parameters of flow rate (viscous forces) and initial condition. From these experiments, four critical observations result, each of which we explore in depth below. First, the invasion of individual initially dry fracture intersections follows a repeated dynamic that tends to create a local pool and finger structure, with filled nonconducting horizontal fractures on either side of the intersection (section 4.1). Second, these local structures are primarily linked vertically to form a "slender-ladder" structure. At all flow rates, and for both reinvasion experiments, flow exited the network from a single fracture at the bottom (section 4.2). Third, pulsation in finger zones and larger-scale cascade events occur, but only at low flow. At higher-flow rates, the flow along the pathway is stabilized. For flows such as in our experiment, that do not exceed positive pressure (i.e., unsaturated or tension saturated conditions), only minor additional connections are created as flow rate is increased (section 4.3). Fourth, there is a strong tendency for the current or initial phase structure to guide flow and cause pathways to persist, at least over the time periods of our experiment. However, for low-flow conditions, the possibility remains that pulsation can create new flow paths in time (section 4.4).

4.1. General Intersection Invasion Process Under Initially Dry Conditions

[23] To analyze the general intersection invasion process under initially dry conditions, we will simply consider fractures as filling and emptying at two different pressures given in terms of head (units of length), one for wetting, Ψ_{cf}, and one for draining, Ψ_{df}. These two values are inherently negative, with $\Psi_w > \Psi_d$. Hysteresis could be the result of contact angle differences between wetting and drainage, in-plane curvature influences of the local aperture field [*Glass et al.*, 1998], simple correlation within the local aperture field (an equivalent of the ink bottle effect), or a combination of all three. Let us also consider that, because intersections act as capillary barriers, their values for wetting, Ψ_{wb}, and draining, Ψ_{db}, are different from those of the fractures, with at least $\Psi_{wb} > \Psi_{wf}$.

[24] In the first step of the intersection invasion process, a downward growing finger reaches the capillary barrier formed by the fracture intersection. Because pressure in the finger is less than that required to enter the barrier ($\Psi_{wb} > \Psi_{wf}$), water begins to pool above the intersection. As a pool grows upward, pressure builds at the intersection. Considering the influence of gravity within the pool and neglecting viscous forces, when the intersection breaches, the maximum pool height, h_{pmax}, will be given by:

$$h_{p\max} \approx \Psi_{wb} - \Psi_{wf} \tag{1}$$

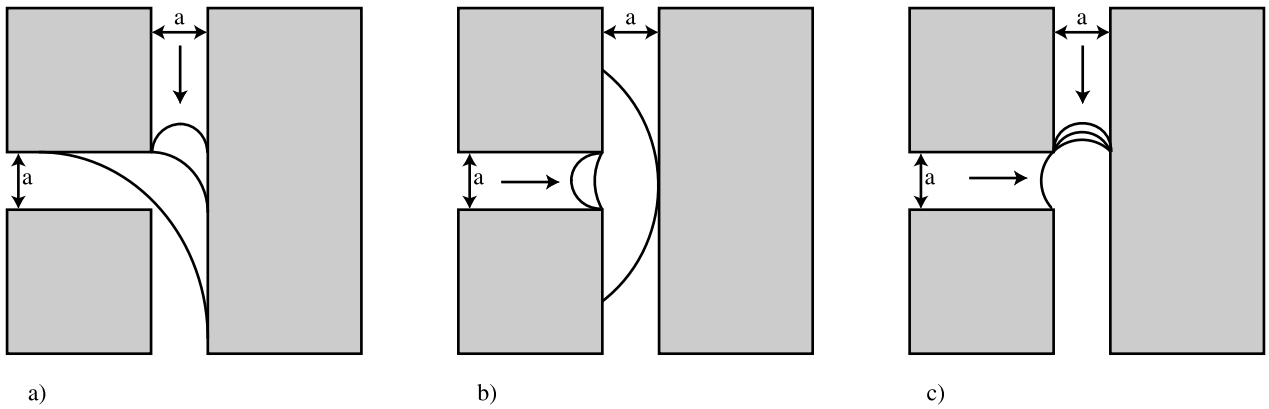

Figure 6. Two-dimensional idealized geometry for phase invasion at a fracture intersection: (a) T intersection, invasion from above throughgoing fracture; (b) T intersection, invasion from side abutting fracture; (c) T intersection, horizontal fracture initially wet or invasion from both horizontal and vertical. Aperture (a) of all fractures is identical.

Once the barrier is breached, water enters the adjoining fractures and the pressure at the growing front immediately reduces to Ψ_{wf}. If $\Psi_{db} < \Psi_{wf}$, the barrier remains open. If not, the barrier will empty after a pulse of water has moved across. Pressure will then build again, followed by breach at Ψ_{wb}, with subsequent pressure lowering and barrier emptying after another small pulse. For a vertical fracture where the pulses can migrate downward and away, this process could carry on indefinitely. For a horizontal fracture, once it fills entirely to an adjoining intersection, pressure will eventually be pushed above Ψ_{db}, thus removing the pulsation. Note that we cannot compare (1) directly to experimental measurements because Ψ_{db} is unknown.

[25] If the barrier remains open (i.e., $\Psi_{db} < \Psi_{wf}$), pool height will decrease if the pressure at the top of the pool reduces below Ψ_{df}. Let us consider first that water only enters the horizontal fracture so that Ψ_{wf} is maintained at the intersection. Including the influence of gravity within the pool and once again neglecting viscous forces, the pool height after drainage, h_{pdrain}, is given by:

$$h_{pdrain} \approx \Psi_{wf} - \Psi_{df} \tag{2}$$

Measured values for both pool heights (~2 cm) and calculated using measurements of Ψ_{wf} and Ψ_{df} (~2 cm) confirm this result. If the water enters the fracture below, it imposes a hanging column, h_{below}, and thus (2) is modified:

$$h_{pdrain} \approx \Psi_{wf} - \Psi_{df} - h_{below} \tag{3}$$

If the next intersection is near, such as we had in our experiment between the two adjoining T subintersections, then h_{below} will be curtailed to a small value. However, for the second T of the intersection, this will not always be the case. As a finger grows downward, its hanging column will increase the likelihood that pool height will continue to decrease below that given by (2). In addition, this hanging column decreases the pressure at the intersection. Such a decrease can halt the invasion of the horizontal fracture, as well as possibly exceed Ψ_{bd}, thus causing the barrier to empty and likely begin to pulsate. However, viscous forces can also come into play to curtail the decrease in pressure at the intersection. We observed in the experiment that as fingers grew downward, they always narrowed a distance behind their tips. This narrowing increases the viscous loss within the finger and can compensate for gravity forces within the hanging column of a finger. In our experiment, all of these possible situations occurred as the lower T at an intersection was spanned and a finger grew downward. However, on most occasions the pool height did not decrease below that given by (2), and thus the influence of the hanging column was curtailed, either due to exceeding Ψ_{bd}, or due to increased viscous forces within the finger. Finally, while not the case in our experiments, we note that if h_{pdrain} is not less than h_{pmax}, pool height above an intersection will not decrease.

4.2. Formation of a Vertical Slender-Ladder Phase Structure

[26] At breakthrough, the repeated action of the general intersection invasion process created a slender-ladder phase structure within the network. If we consider the specifics of the invasion pressure for the offset or T subintersection geometry, such as we had in our experiment (see Figure 6), this network-scale behavior emerges directly. Assuming a two-dimensional configuration with sharp corners and a near zero contact angle, if we invade the intersection from the throughgoing fracture (top or bottom in our experiment), then Ψ_{wb} will be given by the curvature of the air-water meniscus when it touches the lower left hand intersection corner (see Figure 6a):

$$\Psi_{wb} \approx \frac{1-\sqrt{2}}{\sqrt{2}} \frac{\sigma}{\rho g a} \tag{4}$$

In equation (4), σ is the interfacial tension, ρ the density of water, and a the fracture aperture. However, if we invade the T from the abutting fracture (horizontal in our experiment) we see that zero pressure at least is required for entry because the meniscus must pass through a stage where it is flat (see Figure 6b). For near zero contact angles, film flow down the edge of the fracture may occur at near zero pressures. For greater contact angles (such as shown in Figure 6b), the gap will span at positive pressure when the

convex meniscus touches the far side of the throughgoing fracture. While not present in our experiment, we note that a perfect, symmetrical, expanded cross intersection (similar to the idealized pores studied by *Li and Wardlaw* [1986, Figure 12]) does not yield a similar directional dependence of breach pressure.

[27] Because a higher pressure is required to invade the T intersection from the abutting fracture than from the throughgoing fracture, throughgoing fractures act as capillary barriers to flow in abutting fractures. Within the context of our experiment, this action tended to create a phase structure that resembled a slender vertical ladder (single vertical with horizontals on either side). Importantly, the barrier action of the vertical throughgoing fractures was maintained as the flow rate through the pathway increased. Thus under tension saturated conditions as we likely had at our highest flow rate within most of the network, the pathway maintains its slender-ladder structure.

4.3. Network-Scale Dynamic Behavior

[28] Our experiment demonstrated both dynamic and steady behaviors at low-flow rate. Both in the first 7.5 hours of the initial infiltration and across the 17 days of the low-flow reinvasion, we saw individual pulsations as well as cascade events where a number of pulsating fractures acted in concert. Pulsation in finger zones at low-flow rate can be understood by extending our hanging column argument from section 4.1 beyond the single intersection. Neglecting viscous forces, the liquid phase structure must eventually fragment and begin to pulsate as it grows in the vertical. Within our network, this occurred primarily within regions spanned by a finger, usually at or just below the lower T subintersection. If different hanging columns are required for each break point and if these columns vary slightly in time due to dynamic processes (e.g., inertial effects, contact angle dynamics, etc.), one can easily imagine a configuration where connecting and snapping tendrils could lead to a possibly nonrepeating dynamic. The organization of this dynamic into a cascade event can occur when individual pulses become synced. We know from study of the drainage process, that without flow, the finger zones cannot support themselves, and eventually snap (see section 3.3). So, if a break interrupts flow for a sufficient length of time, some tendrils below will snap as well. If water is ''resupplied'' by the next pulse before a given tendril snaps, then it will remain connected. Thus cascade events are likely controlled by a single dominant pulsation point.

[29] During the latter half of the initial low-flow infiltration, the unsteady dynamic was replaced with a steady, nonpulsating configuration. Such a steady configuration may have come about through a very small reconfiguration of the phase structure that increased the local viscous pressure drop at one or more pulsation points. If we recognize that little viscous pressure drop occurs within pools or in horizontal fractures filled to their full width, the viscous drops across these narrow critical pulsation points could become quite large, and thus compensate for the hanging column.

4.4. Persistence and the Guiding of Flow by the Existing Phase Structure

[30] At least at the timescale of our experiment, the existing (initial or current) phase structure tends to guide persistent flow within the fracture network. This is primarily due to the hysteretic behavior of the intersections. During steady, nonpulsating flow conditions, fracture intersections remain open (breached) and the flow pathway persists. During reinvasion of the prewet and drained (stagnant) network, the fact that we did not see any pool height changes before intersections passed water (both low- and high-flow rate) suggests that either the fracture intersections remained open after drainage, or alternatively, their entry pressure was greatly reduced. The first of these could occur if Ψ_{bd} was not achieved during drainage before the tendril below snapped and isolated the intersection. Alternatively, the entry pressure of the barrier could be reduced if at least two fractures at the intersection remain filled with water. For this second case, invasion of the intersection is facilitated such as seen in pores wetting from multiple necks [e.g., *Li and Wardlaw*, 1986; *Glass and Yarrington*, 1996]. For this case, water enters and fills the intersection when interfaces touch (see Figure 6c). Given a two-dimensional configuration with zero contact angle, Ψ_{wb} becomes:

$$\Psi_{wb} \approx \frac{-2}{\sqrt{2}} \frac{\sigma}{\rho g a} \tag{5}$$

[31] Thus, compared to that of the initially dry fracture intersection given by equation (4), invasion of the prewetted fracture is facilitated by a factor of nearly 5. Note also that this mechanism removes the directional dependence of the invasion pressure, and thus in combination with the invasion pressure reduction, it can impart significant hysteresis. More generally, such a facilitation mechanism will also act to reduce entry pressures during initial wetting if more than one fracture is feeding an intersection. Finally, we note that this same facilitation mechanism can operate under prewetted and multiple feed conditions for the perfect, symmetrical, nonoffset expanded cross intersection as well.

[32] If we consider the low-flow reinvasion experiment, an exception to ''flow path guidance by past history'' seems to occur. In this experiment, the invasion process avoids the D fracture below D5 and instead moves to the right to invade initially dry intersections within the E fracture (see Figure 5c). However, on close inspection we see that during the previous high-flow reinvasion experiment, the intersection at E4 was wetted. Since two of the three fractures that join at E4's T intersection were initially wet, the difference between the invasion pressures at the intersection for throughgoing and abutting fractures vanishes. Invasion pressures at both D4 and E4 now being equal, because the E4 intersection is slightly below D4, E4 will be preferred for invasion when viscous forces are negligible (low flow rates). As an aside, we note that the invasion of peripheral T intersections from the abutting fracture during the high-flow reinvasion experiment suggests that higher pressures were achieved during reinvasion than during the sequential increasing of flow rate. This is not surprising because a hanging column below the primary intersection along the developing slender-ladder structure had yet to form at the time these peripheral T intersections were invaded. Such a hanging column existed in full when the flow was increased to this same rate at the end of the increasing flow sequence.

[33] Finally, during periods of unsteady or pulsating flow, an intersection may open and close. In most cases during

pulsation the pathway persisted, but, during the final low-flow reinvasion experiment, an additional pathway was formed from above the lowest pulsation point (see purple zone in Figure 5c). While this new pathway reconnected to the main conducting structure and stagnated, it could just as easily have spanned the network and possibly redirected the outflow.

5. Concluding Remarks

[34] Our experiment and subsequent analyses demonstrate the critical control of fracture intersections as water infiltrates through an unsaturated fracture network within an impermeable matrix. Many of our results can be understood as direct extensions of the behavior of individual fractures to fracture networks as hypothesized by *Glass et al.* [1995]. Similar behavior has been alluded to in field experiments [e.g., *Faybishenko et al.*, 2000; *Glass et al.*, 2002b], and suggested by mesoscale fracture-matrix network experiments in the laboratory [*Glass et al.*, 2002a]. Our results are also similar in many respects to those obtained in heterogeneous sand systems containing sequences of capillary barriers. In these granular systems, the invading phase also pools above capillary barriers and fingers below for both wetting fluid invasion, where fingers have been documented to go through a single pulse at the finger tip [e.g., *Glass and Nicholl*, 1996], and nonwetting fluid invasion, where pulsation both in the pools and within individual fingers has been recently documented [e.g., *Glass et al.*, 2000].

[35] When initially dry, fracture intersections in our network behave as capillary barriers and yield a repeated dynamic as each intersection is spanned. The main flow pathway evolves as a structure composed of pools joined by fingers with occasional expanses of horizontal fracture spanned to full width. Off the main pathway, horizontal fractures form branches that do not conduct, but remain hydraulically connected, and thus can play a role for transport as diffusive sinks. Analysis of the directional dependence of the breach pressure at an offset fracture intersection demonstrates that this ''slender-ladder'' phase structure emerges at the system-scale as a direct consequence of the local intersection invasion process. Even at high-flow rates where the structure becomes tension saturated, the slender-ladder structure is preserved. If offset intersections of the type considered here are ubiquitous in nature, then the emergent slender ladder structure may dominate unsaturated flow in fracture networks, leading to rapid and deep penetration by infiltrating water.

[36] Pulsation at intersections, within fingers, and along horizontal fractures occurs at low steady flow rates, but is stabilized by viscous forces at higher-flow rates. When pulsation occurs, the temporal dynamic sometimes includes cascade events with several locations acting in concert. This unsteady dynamic can also be replaced by a steady, non-pulsating state. At this point, we can only speculate as to why one state is preferred over another at any given time. However, operating at increasing scales, such cascade events could easily account for the large fluctuations seen in the outflow of the mesoscale fracture-matrix experiments of *Glass et al.* [2002a]. Pathway switching was also noted in these earlier mesoscale experiments. While we also found pathway switching at low flow and in context of pulsation, it played a relatively minor role, at least at the timescales of our experiment.

[37] During reinvasion, intersections in the drained, stagnant initial state do not behave as capillary barriers. The fracture network is rapidly spanned, with fingers growing sequentially below each intersection. This suggests that fracture intersections have a dramatic hysteretic response. When initially dry, they wet under near zero pressure. When the intersection is prewet, they are either initially filled with water or their invasion is facilitated to fill at pressures comparable to those of the fractures. This hysteretic behavior shows the importance of the initial phase structure to guide the invasion process and thus emphasizes the critical importance of history.

[38] Finally, while one expects single and double T intersections, as well as their nonorthogonal relatives, to be pervasive in nature, their juxtaposition will likely be far less regular than in our experiment. Natural fracture sets will be three-dimensional, and are likely to exhibit inclinations that differ from the strict vertical-horizontal orientations considered in our two-dimensional model. Also, the inherent aperture and topologic variability within individual fractures is expected to influence behavior at intersections. Finally, one expects some intersections will be bridged with loose material (rock, soil) that may lower their breach pressure from the ''clean'' or ''open'' value. We expect that all of these increased degrees of freedom will influence system behavior, and could combine to cause either enhanced flow convergence or divergence at both the local and macro scales. Consideration of the behavior of individual fracture intersections, as well as their assembly within the context of a fracture network, promises to be an area of fertile research.

[39] **Acknowledgments.** These experiments were conducted in 1997 at the Flow Visualization and Processes Laboratory, Sandia National Laboratories, with support from the U.S. Department of Energy's Basic Energy Sciences Geoscience Research Program under contract DE-AC04-94AL85000. Data analysis and the writing of this manuscript were supported by the U.S. Department of Energy's Environmental Management Science Program under contract DE-AC04-94AL85000 at Sandia National Laboratories, DE-FG07-02ER63499 at the University of Idaho, DE- FG07-02ER63514 at the University of Colorado, and DE-AC07-99ID13727 at the Idaho National Engineering and Environmental Laboratory. We would also like to thank Justin von Deming, Lee Orear, and Don Fox for their aid in constructing and maintaining the experiments.

References

Amundsen, H., G. Wagner, U. Oxaal, P. Meakin, J. Feder, and T. Jossang, Slow two-phase flow in artificial fractures: Experiments and simulations, *Water Resour. Res.*, *35*(9), 2619–2626, 1999.

Dahan, O., R. Nativ, M. Adar, B. Berkowitz, and Z. Ronen, Field observation of flow in a fracture intersecting unsaturated chalk, *Water Resour. Res.*, *35*(11), 3315–3326, 1999.

Davidson, G. R., R. L. Bassett, E. L. Hardin, and D. L. Thompson, Geochemical evidence of preferential flow of water through fractures in unsaturated tuff, Apache Leap, Arizona, *Appl. Geochem.*, *13*(2), 185–195, 1998.

Fabryka-Martin, J. T., P. R. Dixon, S. S. Levy, B. Liu, D. L. Brenner, L. E. Wolfsberg, H. J. Turin, and P. Sharma, Implications of environmental isotopes for flow and transport in the unsaturated zone at Yucca Mountain, Nevada, *Geol. Soc. Am. Abstr. Programs*, *28*(7), A-416, 1996.

Faybishenko, B., C. Doughty, S. Steiger, J. Long, T. Wood, J. Jacobsen, J. Lore, and P. Zawislanski, Conceptual model of the geometry and physics of water flow in a fractured basalt vadose zone, *Water Resour. Res.*, *36*(12), 3499–3520, 2000.

Glass, R. J., and M. J. Nicholl, Physics of gravity fingering of immiscible fluids within porous media: An overview of current understanding and selected complicating factors, *Geoderma*, *70*, 133–163, 1996.

Glass, R. J., and L. Yarrington, Simulation of gravity-driven fingering in porous media using a modified invasion percolation model, *Geoderma*, *70*, 231–252, 1996.

Glass, R. J., M. J. Nicholl, and V. C. Tidwell, Challenging models for flow in unsaturated, fractured rock through exploration of small scale flow processes, *Geophys. Res. Lett.*, *22*(11), 1457–1460, 1995.

Glass, R. J., M. J. Nicholl, and L. Yarrington, A modified invasion percolation model for low capillary number immiscible displacements in horizontal rough walled fractures: Influence of local in-plane curvature, *Water Resour. Res.*, *34*(12), 3215–3234, 1998.

Glass, R. J., S. H. Conrad, and W. Peplinski, Gravity destabilized nonwetting phase invasion in macroheterogeneous porous media: Experimental observations of invasion dynamics and scale analysis, *Water Resour. Res.*, *36*(11), 3121–3137, 2000.

Glass, R. J., H. Rajaram, M. J. Nicholl, and R. L. Detwiler, The interaction of two fluid phases in fractured media, *Curr. Opinion Colloid Interface Sci.*, *6*, 223–235, 2001.

Glass, R. J., M. J. Nicholl, S. E. Pringle, and T. R. Wood, Unsaturated flow through a fracture-matrix network: Dynamic preferential pathways in mesoscale laboratory experiments, *Water Resour. Res.*, *38*(12), 1281, doi:10.1029/2001WR001002, 2002a.

Glass, R. J., M. J. Nicholl, A. L. Ramirez, and W. D. Daily, Liquid phase structure within an unsaturated fracture network beneath a surface infiltration event: Field experiment, *Water Resour. Res.*, *38*(10), 1199, doi:10.1029/2000WR000167, 2002b.

Kneafsey, T. J., and K. Pruess, Laboratory experiments on heat-driven two-phase flows in natural and artificial rock fractures, *Water Resour. Res.*, *34*(12), 3349–3367, 1998.

Li, Y., and N. C. Wardlaw, Mechanisms of nonwetting phase trapping during imbibition at slow rates, *J. Colloid Interface Sci.*, *109*(2), 473–486, 1986.

National Research Council, Two-phase immiscible fluid flow in fractures, in *Rock Fractures and Fluid Flow: Contemporary Understanding and Application*, pp. 127–132, 153–160, Natl. Acad. Press, Washington, D. C., 1996.

Nicholl, M. J., R. J. Glass, and H. A. Nguyen, Small-scale behavior of single gravity-driven fingers in an initially dry fracture, *High Level Radioact. Waste Manage.*, *4*, 2023–2032, 1993a.

Nicholl, M. J., R. J. Glass, and H. A. Nguyen, Wetting front instability in an initially wet unsaturated fracture, *High Level Radiat. Waste Manage.*, *4*, 2061–2070, 1993b.

Persoff, P., and K. Pruess, Two-phase flow visualization and relative permeability measurement in rough-walled fractures, *Water Resour. Res.*, *31*(5), 1175–1186, 1995.

Podgorney, R. K., T. R. Wood, B. Faybishenko, and T. M. Stoops, Spatial and temporal instabilities in water flow through variably saturated fractured basalt on the one-meter field scale, in *Dynamics of Fluids in Fractured Rock*, *Geophys. Monogr. Ser.*, vol. 122, pp. 129–146, AGU, Washington, D. C., 2000.

Russell, C. E., J. W. Hess, and S. W. Tyler, Hydrogeologic investigation of flow in fractured tuffs, Rainier Mesa, Nevada Test Site, in *Flow and Transport Through Unsaturated Fractured Rock*, *Geophys. Monogr. Ser.*, vol. 42, edited by D. D. Evans and T. J. Nicholson, pp. 43–50, AGU, Washington, D. C., 1987.

Su, G. W., J. T. Geller, K. Pruess, and F. Wen, Experimental studies of water seepage and intermittent flow in unsaturated, rough-walled fractures, *Water Resour. Res.*, *35*(4), 1019–1037, 1999.

Su, G. W., J. T. Geller, K. Pruess, and J. R. Hunt, Solute transport along preferential flow paths in unsaturated fractures, *Water Resour. Res.*, *37*(10), 2481–2491, 2001.

Wood, T. R., M. J. Nicholl, and R. J. Glass, Fracture intersections as integrators for unsaturated flow, *Geophys. Res. Lett.*, *29*(24), 2191, doi:10.1029/2002GL015551, 2002.

R. J. Glass, Flow Visualization and Processes Laboratory, Sandia National Laboratories, Mail Stop 0735, Albuquerque, NM 87185-0735, USA. (rjglass@sandia.gov)

M. J. Nicholl, Mining and Geological Engineering, University of Idaho, Moscow, ID 83843, USA. (mnicholl@uidaho.edu)

H. Rajaram, Department of Civil, Environmental, and Architectural Engineering, University of Colorado, Boulder, CO 80309, USA. (hari@colorado.edu)

T. R. Wood, Idaho National Engineering and Environmental Laboratory, Idaho Falls, ID 83415, USA. (tqw@inel.gov)